On the Relation of the Dynamic Behavior between the Two Diastereomers of the Linear Tetranuclear Ruthenium Cluster $Ru_4(CO)_{10}[CH_3C{=}C(H)C(H){=}N\text{-}i\text{-}Pr]_2$ and Their Isolobal Counterparts $[\eta^5\text{-}CpM(CO)_2]_2$ (M = Fe, Ru)[1]

Wilhelmus P. Mul,[†] Jan-Meine Ernsting,[†] Wim G. J. de Lange,[†] Mark D. M. van Straalen,[†] Kees Vrieze,[†] Cornelis J. Elsevier,*[,†] Martin de Wit,[‡] and Casper H. Stam[‡]

Contribution from the Anorganisch Chemisch Laboratorium, Universiteit van Amsterdam, J. H. van't Hoff Instituut, Nieuwe Achtergracht 166, 1018 WV Amsterdam, The Netherlands, and Laboratorium voor Kristallografie, Universiteit van Amsterdam, J. H. van't Hoff Instituut, Nieuwe Achtergracht 166, 1018 WV Amsterdam, The Netherlands. *Received May 18, 1992*

Abstract: The two diastereomers of the linear tetranuclear cluster $Ru_4(CO)_{10}[CH_3C{=}C(H)C(H){=}N\text{-}i\text{-}Pr]_2$, (CA/AC)-(**1a**) and (CC/AA)-**1a**, have been separated by preparative HPLC. Two different modes for diastereomer interconversion have been assessed; a thermally induced isomerization which proceeds *intermolecularly*, and a CO induced isomerization which occurs *intramolecularly*, as could be shown employing labeling experiments. Both diastereomers can exist in cis and trans configurations. The X-ray crystal structure of *cis*-(CC/AA)-**1a** has been solved. The molecule exhibits (noncrystallographic) C_2 symmetry and contains two mutually cis-disposed η^5-azaruthenacyclopentadienyl fragments coordinated to a central $Ru_2(CO)_2(\mu\text{-}CO)_2$ unit. In the solid state of samples obtained by various methods all configurations (i.e., *cis*-(CA/AC)-**1a**, *trans*-(CA/AC)-**1a**, *cis*-(CC/AA)-**1a**, *trans*-(CC/AA)-**1a**) have been observed by IR spectroscopy in KBr. In solution at room temperature both (CA/AC)-**1a** and (CC/AA)-**1a** undergo rapid cis/trans isomerization and bridge/terminal exchange of the CO ligands of the central $Ru_2(CO)_2(\mu\text{-}CO)_2$ unit. At low temperature (183 K) these processes, except the bridge/terminal exchange for *trans*-(CC/AA)-**1a**, are slow on the NMR time scale. Hence, it has been established for the first time for bis(dicarbonyl-(pseudo)cyclopentadienylruthenium) complexes that cis/trans and bridge/terminal CO exchange can be two independent processes. A rationale for the different kinetic barriers for bridge/terminal CO exchange in the trans configurations of the (CA/AC) and (CC/AA) diastereomers of **1a**, based on the diastereomeric nature of the complexes and intermediates, is given.

Introduction

The dynamic behavior of ligands in organometallic complexes is of considerable interest, not only from a theoretical point of view but also because ligand fluxionality or mobility and (catalytic) reactivity are interrelated.[2] The interconversion of the cis and trans isomers of $[CpM(CO)_2]_2$ (M = Fe, Ru) in solution, as shown in Figure 1, represents a classic example of fluxional behavior of a metal-carbonyl complex. This process, as formulated by Adams and Cotton,[3] is believed to proceed by pairwise opening of the CO bridges to give a nonbridged isomer, rotation about the metal-metal bond, and pairwise reclosing of the CO bridges.

At room temperature cis/trans isomerization in $[CpFe(CO)_2]_2$ is fast on the NMR time scale, giving rise to only one resonance for the Cp protons. At −70 °C, however, cis/trans isomerization is slow on the NMR time scale and two resonances are observed for the Cp protons, which have been assigned to the cis and trans isomers of $[CpFe(CO)_2]_2$.[4] The corresponding low-temperature ^{13}C NMR spectrum shows static CO ligands in the cis isomer, whereas rapid exchange of the terminal and bridging CO ligands takes place in the trans isomer.[5] To account for the much more facile bridge/terminal CO exchange in the trans isomer, the geometries of the intermediate nonbridged isomers have to be considered.[3] The concerted pairwise opening of the CO bridges in the trans isomer leads to the most easily accessible, noneclipsed intermediate, which is shown in Figure 2a, in which all four CO ligands are equivalent. Then, without any internal rotation, bridges may be reformed using CO groups which were previously either in terminal or in bridging positions.

The cis isomer may lead to either of the nonbridged intermediates **b** and **c** shown in Figure 1. As the CO ligands in both **b** and **c** are nonequivalent, only those CO ligands that were initially in bridging position can form a pair of bridges again, without internal rotation being necessary. For bridge/terminal CO exchange, rotation of one $CpFe(CO)_2$ unit by 2 × 120° with respect to the other must take place in the nonbridged tautomers (i.e., **b** and **c**), which process requires energy and therefore slows bridge/terminal CO exchange in the cis isomer relative to the trans isomer.[6] In solution varying amounts of both isomers of $[CpFe(CO)_2]_2$ are present, the cis isomer being favored in more polar solvents, whereas, according to Manning, a nonbridged isomer is "only detectable under most favorable conditions".[7]

Gansow and co-workers have investigated the fluxional behavior of $[CpRu(CO)_2]_2$ and some derivatives thereof by NMR.[5] It was found that cis/trans isomerization for $[CpRu(CO)_2]_2$ ($\Delta G^{\ddagger}$ = 29.4 kJ mol^{-1}) was more facile than for $[CpFe(CO)_2]_2$ ($\Delta G^{\ddagger}$ = 52.1 kJ mol^{-1}) and that sizable amounts of nonbridged isomers of $[CpRu(CO)_2]_2$ are present in solution at higher temperatures.[5,8]

* To whom correspondence should be addressed.

(1) Reactions of Monoazadienes with Metal Carbonyl Complexes. Part IX. For other parts see refs 10, 11, 13, 17, and 22. See also: Elsevier, C. J.; Mul, W. P.; Vrieze, K. *Inorg. Chim. Acta* **1992**, *198-200*, 689-703.

(2) (a) Vahrenkamp, H. *Struct. Bonding* **1977**, *32*, 1. (b) Cotton, F. A. *Bull. Soc. Chim. Fr.* **1973**, 2587. (c) Band, E.; Meutterties, E. L. *Chem. Rev.* **1978**, *78*, 639. (d) Mlekuz, M.; Bougeard, P.; Sayer, B. G.; Peng, S.; McGlinchey, M. J.; Marinetti, A.; Saillard, J.-Y.; Naceur, J. B.; Mentzen, B.; Jouen, G. *Organometallics* **1985**, *4*, 1123. (e) *Dynamic Nuclear Magnetic Resonance Spectroscopy*; Jackman, L. M., Cotton, F. A., Eds.; Academic Press: New York, 1975; pp 253-522. (f) Johnson, B. F. G.; Benfield, R. E. In *Transition Metal Clusters*; Johnson, B. F. G., Ed.; Wiley-Interscience: Chicester 1980; 471. (g) Cotton, F. A. *J. Organomet. Chem.* **1975**, *100*, 29. (h) Faller, J. W. *Adv. Organomet. Chem.* **1976**, *17*, 211. (i) Evans, J. *Adv. Organomet. Chem.* **1976**, *17*, 319.

(3) Adams, R. D.; Cotton, F. A. *J. Am. Chem. Soc.* **1973**, *95*, 6589.

(4) (a) Bullitt, J. G.; Cotton, F. A.; Marks, T. J. *J. Am. Chem. Soc.* **1970**, *92*, 2155. (b) Bullitt, J. G.; Cotton, F. A.; Marks, T. J. *Inorg. Chem.* **1972**, *11*, 671.

(5) (a) Gansow, O. A.; Burke, A. R.; Vernon, W. D. *J. Am. Chem. Soc.* **1972**, *94*, 2550. (b) Gansow, O. A.; Burke, A. R.; Vernon, W. D. *J. Am. Chem. Soc.* **1976**, *98*, 5817.

(6) (a) Fehlammer, W. P.; Stolzenberg, H. in *Comprehensive Organometallic Chemistry*; Wilkinson, G., Stone, F. G. A., Abel, E. W., Eds.; Pergamon Press: Oxford, 1982; Vol. 4, p 513. (b) Farrugia, L. J.; Mustoo, L. *Organometallics* **1992**, *11*, 2941.

(7) Manning, A. R. *J. Chem. Soc. A* **1968**, 1319.

0002-7863/93/1515-980$04.00/0

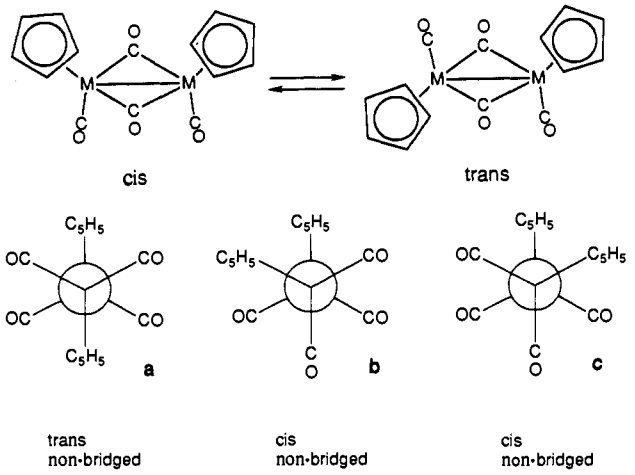

Figure 1. Interconversion between cis and trans isomers of $[CpM(CO)_2]_2$ and Newman projections of the nonbridged intermediates in fluxional $[CpFe(CO)_2]_2$.

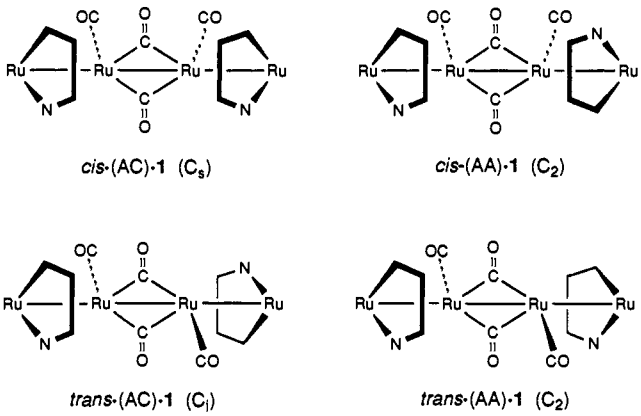

Figure 2. Configurations of $Ru_4(CO)_{10}[CH_3C{=}C(H)C(H){=}N\text{-}i\text{-}Pr]_2$ (**1a**) with point group designation in parentheses.

Based on low-temperature ^{13}C NMR spectra it was concluded that, in contrast to the iron analogue, bridge/terminal interconversion and cis/trans isomerization in $[CpRu(CO)_2]_2$ occur simultaneously.[9]

Recently, we have isolated a series of linear tetranuclear ruthenium clusters, $Ru_4(CO)_{10}[R^1C{=}C(H)C(H){=}NR^2]_2$ (R^1,R^2 = CH_3,*i*-Pr (**1a**), CH_3,c-Hex (**1b**), CH_3,*t*-Bu (**1c**), C_6H_5,*i*-Pr (**1d**), C_6H_5,*t*-Bu (**1e**)) containing two β-metalated monoazadien-4-yl ligands, in good yield from thermal reactions of $Ru_3(CO)_{12}$ with monoazadienes ($R^1C(H){=}C(H)C(H){=}NR^2$; abbreviated as R^1,R^2-MAD).[10-12] The cluster $Ru_4(CO)_{10}[R^1C{=}C(H)C(H){=}NR^2]_2$ may be envisaged as an isolobal analogue of $[CpM(CO)_2]_2$ (M = Fe, Ru),[10] and it has been shown that the formation of **1a-e** proceeds via organometallic compounds related to those in the formation of $[CpM(CO)_2]_2$.[11,13] Its isolobal relationship with $[CpM(CO)_2]_2$ led to question whether cis/trans isomerization also takes place in solution for **1**.

The clusters **1a-e** can exist, due to the presence of two chiral η^5-azaruthenacyclopentadienyl units, in two diastereomeric forms, (CA/AC)-**1** and (CC/AA)-**1**,[14] which do not readily interconvert at room temperature.[11,15] Furthermore, each diastereomer may be present in the cis or trans configuration, hence, four carbonyl-bridged enantiomeric pairs may be anticipated (see Figure 2). By virtue of the chiral azaruthenacycles, the bridging CO ligands in *cis*-(CA/AC)-**1** and *trans*-(CC/AA)-**1** are inequivalent, which may enable one to distinguish between the energy barriers of cis/trans isomerization and CO bridge/terminal exchange in these diastereomers.

Experimental Section

Materials and Apparatus. ^1H and $^{13}C\{^1H\}$ NMR spectra were obtained on Bruker AC100, WM250, and AM500 spectrometers. IR spectra were recorded with a Nicolet 7199B FT-IR interferometer using a matched NaCl solution cell of 0.5 mm path length and electronic absorption spectra on a Perkin-Elmer Lambda 5 UV-vis spectrophotometer. The field desorption (FD) mass spectrum[16] was obtained with a Varian MAT-711 double focussing mass spectrometer with a combined EI/FI/FD source, fitted with a 10-μm tungsten wire FD-emitter containing carbon microneedles with an average length of about 30-μm, using emitter currents of 0-15 mA.

Reactions were carried out under an atmosphere of dry nitrogen, unless stated otherwise, by using Schlenk techniques. Solvents used for synthetic purposes were carefully dried and distilled prior to use. Silica gel used for column chromatography (kieselgel 60, 70-230 mesh, E. Merck, Darmstadt, West Germany) was dried before use. $Ru_4(CO)_{10}[CH_3C{=}C(H)C(H){=}NR^2]_2$ (R^2 = *i*-Pr (**1a**), c-Hex (**1b**)) was synthesized as described before.[10,11]

The HPLC separations were performed with a modular Gilson liquid chromatographic system consisting of two 303 elution pumps, an 811 mixing chamber, a 7125 Rheodyne injector equipped with a 20-μL (analytical) or 2-mL (preparative) sample loop, an 802c manometric module, and an 111 B UV detector operated at 254 nm, all obtained from Meyvis, The Netherlands. The system was controlled by an Apple Macintosh SE with Rainin software. Analytical columns: Hypersil ODS 5-μm (100 × 4.8 mm) reversed-phase (RP) column; Lichrosorb Si-60 Å 7-μm (250 × 10.4 mm) normal-phase (NP) silica gel column. Preparative columns: Dynamax-C18 8-μm (250 × 21.4 mm) RP column in combination with a Dynamax-C18 8-μm (50 × 21.4 mm) RP guard column; Dynamax Si-60 Å 8-μm (250 × 21.4 mm) NP column in combination with a Dynamax Si-60 Å 8-μm (50 × 21.4 mm) NP guard column. Eluent: a helium degassed solvent mixture of CH_3OH/H_2O (RP) or hexane/dichloromethane (NP) was used isocratically. The aforementioned preparative columns were purchased from Meyvis, the analytical RP-column from Hewlett-Packard, whereas the analytical silica column was home filled. All samples were filtered over a disposable PTFE syringe filter (25 mm membrane, poresize: 0.45-μm) from Core Palmer Instrument Company before they were passed through an HPLC column.

(8) (a) Fischer, R. D.; Vogler, A.; Noack, K. *J. Organomet. Chem.* **1967**, *7*, 135. (b) Noack, K. *J. Organomet. Chem.* **1967**, *7*, 151.

(9) It should be noted, however, that this conclusion may be argued since it was based on limiting low-temperature ^{13}C NMR spectra of $[CpRu(CO)_2]_2$ and derivatives thereof, which show only one set of signals, one in the bridging CO region and one in the terminal CO region. These signals are proposed to be composed of overlapping resonances of both the cis and trans isomers. Alternatively, however, this low-temperature ^{13}C NMR spectrum can be interpreted as showing static CO ligands in the cis isomer, whereas the CO ligands of the trans isomer are in the intermediate exchange.

(10) Polm, L. H.; Mul, W. P.; Elsevier, C. J.; Vrieze, K.; Christophersen, M. J. N.; Stam, C. H. *Organometallics* **1988**, *7*, 423.

(11) Mul, W. P.; Elsevier, C. J.; Polm, L. H.; Vrieze, K.; Zoutberg, M. C.; Heijdenrijk, D.; Stam, C. H. *Organometallics* **1991**, *10*, 2247.

(12) MAD is used as acronym for monoazadienes in general. In this paper we will use R^1,R^2-MAD when *N*-alkyl-(*E*)-crotonaldimines $CH_3C(H){=}C(H)C(H){=}NR^2$ or *N*-alkyl-(*E*)-cinnamaldimines $C_6H_5C(H){=}C(H){=}C(H)C(H){=}NR^2$ are meant. Metalated at C_β these ligands form the formally monoanionic monoazadien-4-yl (R^1,R^2-MAD-yl) ligand $R^1C^- = C(H)C(H){=}NR^2$. Suffixes to the atoms refer to $R^1C(H)_\beta{=}C(H)_\alpha C(H)_{im}{=}NR^2$.

(13) Spek, A. L.; Duisenberg, A. J. M.; Mul, W. P.; Beers, O. C. P.; Elsevier, C. J. *Acta Crystallogr., Sect. C: Cryst. Struct. Commun.* **1990**, *C47*, 297.

(14) The configurations of the outer (cyclometalated) ruthenium atoms of **1** have been determined according to the Brown-Cook-Sloan modification of the Cahn-Ingold-Prelog rules,[14a] which have recently been recommended by IUPAC.[14b] Throughout this paper the official stereochemical descriptors for the chiral ruthenium atoms, OC-6-33-C and OC-6-33-A, will be abbreviated C and A, respectively.[1] It should be noted that the inner ruthenium atoms of **1** are chiral too, but, since their chirality is related to the chirality of the outer ruthenium atoms, the chirality of the inner ruthenium atoms will be omitted in order to avoid the use of redundant chirality descriptors, i.e., (CA) stands for $[C_{Ru(1)},A_{Ru(4)}]$ and (CC) for $[C_{Ru(1)},C_{Ru(4)}]$. Both diastereomers are formed as 1:1 mixtures of two enantiomers. The (CA) and (AC) enantiomers of the meso compound (CA/AC)-**1** are identical, whereas the (CC) and (AA) enantiomers of (CC/AA)-**1a** are mirror images.[10] (a) Sloan, T. E. In *Topics in Inorganic and Organometallic Stereochemistry*; Geoffroy, G. L., Ed.; Wiley-Interscience: 1981; Vol. 12, p 1. (b) *IUPAC, Nomenclature of Inorganic Chemistry, Recommendations 1990*; Leigh, G. J., Ed.; Blackwell Scientific Publications: Oxford, 1990; pp 171, 186.

(15) Although the clusters **1a-e** are formed as 1:1 mixtures of two diastereomers, the ratios isolated for R^1, R^2 = C_6H_5,*i*-Pr (**1d**), C_6H_5,*t*-Bu (**1e**) differ markedly from unity. This can be ascribed to the thermally induced isomerization (vide infra) with concomitant precipitation of the less soluble diastereomer from hot heptane solutions during their syntheses. In contrast to cis/trans isomerization, diastereomer interconversion is a high-energy process (vide infra).

(16) Schulten, H. R. *Int. J. Mass Spectrosc. Ion Phys.* **1979**, *32*, 97.

HPLC Conditions for Preparative Separation of the Two Diastereomers of 1a and 1b. i. $Ru_4(CO)_{10}[CH_3C{=}C(H)C(H){=}N\text{-}i\text{-}Pr]_2$ (**1a**), preparative NP column; eluent, hexane/CH_2Cl_2 (90:10); flow rate, 10 mL/min; (CA/AC)-**1a**, $t_{r(1)}$ = 39.3 min; (CC/AA)-**1a**, $t_{r(2)}$ = 50.5 min.

ii. $Ru_4(CO)_{10}[CH_3C{=}C(H)C(H){=}N\text{-}c\text{-}Hex]_2$ (**1b**); preparative NP column; eluent, hexane/CH_2Cl_2 (95:5); flow rate, 10 mL/min; first diastereomer, $t_{r(1)}$ = 31.0 min; second diastereomer, $t_{r(2)}$ = 36.1 min.

Thermally Induced Isomerization of (CA/AC)-1a and (CC/AA)-1a. Pure (CC/AA)-**1a** or (CA/AC)-**1a**, obtained as described above, was dissolved in heptane and stirred at reflux for 1.5 h. The solvent was removed under vacuum, and the residue was dissolved in $CDCl_3$. It was shown (^1H NMR) that in both cases isomerization had taken place and that an approximately 1:1 mixture of the (CA/AC) and (CC/AA) diastereomers of **1a** was obtained.

Kinetic Experiment. The isomerization of (CA/AC)-**1a** into a mixture of (CA/AC)-**1a** and (CC/AA)-**1a** was monitored by ^1H NMR in C_6D_6 at 70 °C (0.01 mM solution). The isomerization rate was obtained by following the decrease respectively the increase of the integral for the methyl resonances of the *i*-Pr groups occurring at the higher chemical shift for each of the individual diastereomers ($\delta_{(CA/AC)}$ = 1.11 ppm (d, ^3J = 6.5 Hz), $\delta_{(CC/AA)}$ = 1.17 ppm (d, ^3J = 6.5 Hz)). The isomerization was found to follow first-order kinetics with $k = (2.0 \pm 0.1)\cdot 10^{-5}$ s^{-1} assuming $[(CA/AC)]_e = [(CC/AA)]_e$.

Thermal Reaction of 1a with 1b. A solution of $Ru_4(CO)_{10}[CH_3C{=}C(H)C(H){=}N\text{-}i\text{-}Pr]_2$ (**1a**, mixture of (CA/AC) and (CC/AA) diastereomers, 50 mg, 0.055 mmol) and $Ru_4(CO)_{10}[CH_3C{=}C(H)C(H){=}N\text{-}c\text{-}Hex]_2$ (**1b**, mixture of (CA/AC) and (CC/AA) diastereomers, 54 mg, 0.055 mmol) in 25 mL of heptane was refluxed under an atmosphere of dry nitrogen for 2 h. The solvent was evaporated under vacuum, and the residue was then first purified by column chromatography on silica. The broad red band, which was obtained using diethyl ether as the eluent, was collected, and the solvent was removed under vacuum. The mixture of complexes present was dissolved in 2 mL of methanol and passed through the preparative RP-HPLC column using methanol/water (94:6) as the mobile phase (flow rate: 10 mL/min) and three base line separated fractions (first fraction, 150–180 mL; second fraction, 240–280 mL; third fraction, 400–450 mL) were collected in an 1:2:1 ratio. These fractions contained $Ru_4(CO)_{10}[CH_3C{=}C(H)C(H){=}N\text{-}i\text{-}Pr]_2$ (**1a**, mixture of two diastereomers), the mixed ligand compound $Ru_4(CO)_{10}[CH_3C{=}C(H)C(H){=}N\text{-}i\text{-}Pr][CH_3C{=}C(H)C(H){=}N\text{-}c\text{-}Hex]$ (**1c**, mixture of two diastereomers), and $Ru_4(CO)_{10}[CH_3C{=}C(H)C(H){=}N\text{-}c\text{-}Hex]_2$ (**1b**, mixture of two diastereomers), respectively. Spectroscopic data for $Ru_4(CO)_{10}[CH_3C{=}C(H)C(H){=}N\text{-}i\text{-}Pr][CH_3C{=}C(H)C(H){=}N\text{-}c\text{-}Hex]$ (**1c**, two diastereomers); IR ν(CO) in hexane solution 2067 (s), 2004 (m), 1992 (s), 1950 (w), 1773 (m) cm^{-1}; ^1H NMR δ (multiplicity, integral, assignment) in $CDCl_3$, in ppm relative to $SiMe_4$, less soluble diastereomer between brackets 6.87, 6.78 [6.89, 6.80] (d, d, ^3J = 2.0 Hz, 1 H, 1 H, C*H*=N-*i*-Pr, C*H*=N-c-Hex), 5.09 [5.09] (br s, 2 H, 2 × C=C*H*) 3.54 [3.52] (sept, ^3J = 6.5 Hz, 1 H, NC*H*$(CH_3)_2$), 3.01 [3.01] (br s, 1 H, NC*H*C_5H_{10}), 2.56^0, 2.53^0 [2.56^8, 2.52^3] (s, s, 3 H, 3 H, 2 × CH=CC*H*$_3$), 1.27–1.15 [1.27–1.15] (m, 16 H, NCH(CH_3)$_2$ and NCHC_5H_{10}); FD-mass found *m/e* 944 (calcd *M* = 944; based on the ^{101}Ru isotope).

CO Induced Isomerization of (CA/AC)-1a and (CC/AA)-1a. Pure (CA/AC)-**1a** or (CC/AA)-**1a** (ca. 20 mg) was dissolved in C_6D_6 or $CDCl_3$ (0.6 mL), and the purity was checked by ^1H NMR. This solution was then saturated with CO and, after standing for a period of about 15 min at ambient temperature, reexamined. In all cases, the latter ^1H NMR spectra showed the presence of an approximately 1:1 mixture of both diastereomers of **1a** together with a small amount of $Ru_4(CO)_{12}$-$[CH_3C{=}C(H)C(H){=}N\text{-}i\text{-}Pr]_2$.[17] Without external CO being present no isomerization was observed under similar conditions. Either of the diastereomers of **1b** was also converted into an approximately 1:1 mixture of both diastereomers within 30 min at room temperature in solution (C_6D_6, $CDCl_3$) when saturated with CO.

Reaction of a Mixture of 1a and 1b with CO. A solution of an equimolar mixture of **1a** (mixture of (CA/AC) and (CC/AA) diastereomers, 50 mg, 0.055 mmol) and **1b** (mixture of (CA/AC) and (CC/AA) diastereomers, 54 mg, 0.055 mmol) in benzene (15 mL) was saturated with CO. Samples of this mixture were taken at regular intervals (0.25–1 h) and analyzed by HPLC (analytical RP column). Slow conversion into the CO adducts $Ru_4(CO)_n[CH_3C{=}C(H)C(H){=}NR^2]_2$ (n = 12–14)[16] took place, but no formation of the mixed ligand complex $Ru_4(CO)_{10}[CH_3C{=}C(H)C(H){=}N\text{-}i\text{-}Pr][CH_3C{=}C(H)C(H){=}N\text{-}c\text{-}Hex]$ (**1c**) was observed over a 24-h period.

Preparation and Separation of ^{13}CO-Enriched (CA/AC)-1a and (CC/AA)-1a. A sample of ^{13}CO-enriched (enrichment about 25%) of $Ru_2(CO)_6[CH_3C{=}C(H)CH_2N\text{-}i\text{-}Pr]$ (0.2 g), prepared as described before,[10] was thermally converted into $Ru_4(CO)_{10}[CH_3C{=}C(H)C(H){=}N\text{-}i\text{-}Pr]_2$ (**1a**) as described in the same paper. After workup **1a** was obtained in an approximately 1:1 mixture of the (CA/AC) and (CC/AA) diastereomers in a yield of 0.15 g. HPLC separation on a preparative NP silica column (vide infra) afforded pure, ^{13}CO-enriched samples of the (CA/AC) and (CC/AA) diastereomers of **1a**, which were used for variable temperature ^{13}C NMR measurements.

Crystal Structure Determination of *cis*-(CC/AA)-$Ru_4(CO)_{10}[CH_3C{=}C(H)C(H){=}N\text{-}i\text{-}Pr]_2$. Crystals of the title compound are monoclinic with space group $P2_1/a$ and four molecules in a unit cell of dimensions a = 18.462 (3) Å, b = 12.377 (3) Å, c = 13.639 (3) Å, β = 103.07 (2)°, V = 3035.7 (11) Å^3, μ(Mo Kα) = 19.7 cm^{-1}, d_{calc} = 1.98 g cm^{-3}. A total of 6209 independent intensities were measured on an Enraf-Nonius CAD4F diffractometer using graphite monochromatized radiation ($1 \le \theta \le 26°$; $-22 \le h \le 22$, $0 \le k \le 15$, $0 \le l \le 16$). Of these, 2453 intensities were below the $2.5\sigma(I)$ level and were treated as unobserved. The structure was solved by means of the heavy-atom method. Refinement proceeded through block-diagonal least-squares calculations, anisotropic for Ru, C, N, and O and isotropic for the H atoms which were located in a ΔF synthesis. An empirical absorption correction (DIFABS)[18] was applied and a weighting scheme $w = 1/(4.84 + F_o + 0.022F_o^2)$ was employed. The anomalous scattering of Ru was taken into account, and an extinction correction was applied. The final R value for the 3756 observed reflections was 0.044 (R_w = 0.083). The calculations were carried out by means of XRAY76.[19] The scattering factors were taken from Cromer and Mann[20] and the dispersion correction of Ru from the International Tables for X-ray Crystallography.[21]

Results and Discussion

Recently, we reported the identification and isolation of one of the diastereomers of $Ru_4(CO)_{10}[R^1C{=}C(H)C(H){=}NR^2]_2$ (**1**), whereas mixtures of diastereomers were expected to be formed.[10] Meanwhile, it has become clear that the formerly applied workup procedure affords the less soluble diastereomer selectively. In fact, during thermal reactions of $Ru_3(CO)_{12}$ and R^1,R^2-MAD, the linear tetranuclear clusters $Ru_4(CO)_{10}[R^1C{=}C(H)C(H){=}NR^2]_2$ (**1**) are formed as approximately 1:1 mixtures of two diastereomers in good yields.[11,15] The less soluble, already isolated diastereomer of **1a** possesses the *trans*-(CA/AC) configuration in the crystal structure.[10] The ^1H and ^{13}C NMR spectra of fractions containing mixtures of both diastereomers of **1a** show at room temperature two sets of resonances, each set corresponding to an individual isomer. These data provide no information with respect to the configurations of **1a** in solution nor to the occurrence of cis/trans isomerization. So, the question arises whether rapid cis/trans isomerization takes place in solution at room temperature or that both diastereomers are present in a fixed cis or trans geometry. As by conventional methods only one of the diastereomers of **1a** could be obtained in pure form (vide supra),[22a] separation on preparative scale of the two diastereomers of $Ru_4(CO)_{10}$-$[CH_3C{=}C(H)C(H){=}N\text{-}i\text{-}Pr]_2$ (**1a**) has been effected by preparative HPLC (see Experimental Section).[22b]

Interconversion of the (CC/AA) and (CA/AC) Diastereomers of 1a. The (CC/AA) and the (CA/AC) diastereomers of **1a** do not decompose, and each maintains it stereochemical integrity

(17) Mul, W. P.; Elsevier, C. J.; Vrieze, K.; Smeets, W. J. J.; Spek, A. L. *Organometallics* **1992**, *11*, 1891.

(18) Walker, N.; Stuart, D. *Acta Crystallogr.* **1983**, *A39*, 158.

(19) Stewart, J. M. The XRAY76 System; Tech. Rep. TR466, Computer Science Center: University of Maryland, College Park, MD, 1976.

(20) Cromer, D. T.; Mann, J. B. *Acta Crystallogr.* **1968**, *A24*, 321.

(21) *International Tables for X-ray Crystallography*; Kynoch Press: Birmingham, 1974; Vol. IV.

(22) (a) It has recently been found that (CA/AC)-**1a** shows an enhanced reactivity toward H_2 compared to (CC/AA)-**1a**. Since the hydrogenation product of **1a**, $H_2Ru_4(CO)_8[CH_3C{=}C(H)C(H){=}N\text{-}i\text{-}Pr]_2$, and (CC/AA)-**1a** can be separated by column chromatography on silica, (CC/AA)-**1a** may also be obtained as a pure compound by using this method. See: Mul, W. P.; Elsevier, C. J.; van Leijen, M.; Vrieze, K.; Smeets, W. J. J.; Spek, A. L. *Organometallics* **1992**, *11*, 1877. (b) Both solid samples as well as solutions of pure (CA/AC)-**1a** and (CC/AA)-**1a** differ in color. The (CA/AC) diastereomer is orange/red, whereas the (CC/AA) diastereomer is less intensive colored and has a yellow/orange tinge. This difference in color is not expressed by different positions of the absorption band observed in the visible region of the UV–vis spectra of the pure diastereomers in dichloromethane. A band at 408 nm is observed for each isomer. However, in agreement with the visual perceptions, the ϵ values of the absorption bands differ ($\epsilon_{(CA/AC),408}$ = 2.2 × 10^4 L mol^{-1} cm^{-1}, $\epsilon_{(CC/AA),408}$ = 1.1 × 10^4 L mol^{-1} cm^{-1}).

Table I. Selected Bond Distances (Å) and Bond Angles (deg) Involving Non-Hydrogen Atoms of *cis*-(CC/AA)-**1a**[a]

Ru(1)–Ru(2)	2.706 (1)	Ru(2)–C(14)	2.291 (9)	Ru(4)–C(8)	1.88 (1)
Ru(2)–Ru(3)	2.759 (2)	Ru(2)–C(15)	2.316 (8)	Ru(4)–C(9)	1.95 (1)
Ru(3)–Ru(4)	2.717 (2)	Ru(2)–C(16)	2.369 (8)	Ru(4)–C(10)	1.897 (9)
Ru(1)–C(1)	1.90 (1)	Ru(2)–N(1)	2.268 (6)	Ru(4)–C(23)	2.072 (8)
Ru(1)–C(2)	1.99 (1)	Ru(3)–C(5)	2.011 (7)	Ru(4)–N(2)	2.123 (7)
Ru(1)–C(3)	1.88 (1)	Ru(3)–C(6)	2.119 (8)	C(21)–C(22)	1.42 (1)
Ru(1)–C(16)	2.058 (8)	Ru(3)–C(7)	1.886 (9)	C(22)–C(23)	1.38 (1)
Ru(1)–N(1)	2.145 (7)	Ru(3)–C(21)	2.270 (8)	C(21)–N(2)	1.35 (1)
Ru(2)–C(4)	1.866 (9)	Ru(3)–C(22)	2.298 (9)	C(14)–C(15)	1.41 (1)
Ru(2)–C(5)	2.101 (8)	Ru(3)–C(23)	2.321 (9)	C(15)–C(16)	1.40 (1)
Ru(2)–C(6)	1.995 (8)	Ru(3)–N(2)	2.293 (6)	C(14)–N(1)	1.34 (1)
		The Metal Carbonyl Part			
Ru(1)–Ru(2)–Ru(3)	167.67 (5)		Ru(2)–C(6)–O(6)	144.1 (6)	
Ru(2)–Ru(3)–Ru(4)	172.33 (7)		Ru(3)–C(5)–O(5)	142.1 (6)	
Ru(1)–C(1)–O(1)	176.1 (7)		Ru(3)–C(6)–O(6)	131.3 (6)	
Ru(1)–C(2)–O(2)	171.3 (8)		Ru(3)–C(7)–O(7)	177.5 (7)	
Ru(1)–C(3)–O(3)	179.0 (8)		Ru(4)–C(8)–O(8)	175.5 (9)	
Ru(2)–C(4)–O(4)	177.9 (7)		Ru(4)–C(9)–O(9)	170.0 (9)	
Ru(2)–C(5)–O(5)	133.7 (6)		Ru(4)–C(10)–O(10)	176.6 (7)	
Ru(2)–C(5)–Ru(3)	84.3 (5)		Ru(2)–C(6)–Ru(3)	84.1 (5)	

[a] Esd's in parentheses.

in hexane or benzene solution in the dark at room temperature.[11] It appears that any of the pure diastereomers of **1a** may be converted into a 1:1 mixture of both diastereomers by two different methods. First, heating a solution of (CC/AA)-**1a** or (CA/AC)-**1a** in heptane at reflux for 1.5 h results in complete equilibration, giving mixtures of both (CC/AA)-**1a** and (CA/AC)-**1a** in a 1:1 ratio (eq 1). This thermal isomerization was followed

$$\underset{\text{(CA/AC)-1a}}{\text{(CA/AC)-}Ru_4(CO)_{10}[CH_3C{=}C(H)C(H){=}N\text{-}i\text{-}Pr]_2} \rightleftharpoons \underset{\text{(CC/AA)-1a}}{\text{(CC/AA)-}Ru_4(CO)_{10}[CH_3C{=}C(H)C(H){=}N\text{-}i\text{-}Pr]_2} \quad (1)$$

by ^1H NMR in C_6D_6 and was shown to obey first-order kinetics at 70 °C (k 2.0×10^{-5} s^{-1}). In order to determine whether this process proceeds via an *inter-* or *intramolecular* pathway, a mixture of $Ru_4(CO)_{10}[CH_3C{=}C(H)C(H){=}N\text{-}i\text{-}Pr]_2$ (**1a**, mixture of both diastereomers) and $Ru_4(CO)_{10}[CH_3C{=}C(H)C(H){=}N\text{-}c\text{-}Hex]_2$ (**1b**, mixture of both diastereomers) was treated thermally in a similar way as described above (eq 2). Preparative HPLC

$$\underset{\mathbf{1a}}{Ru_4(CO)_{10}[CH_3C{=}C(H)C(H){=}N\text{-}i\text{-}Pr]_2} + \underset{\mathbf{1b}}{Ru_4(CO)_{10}[CH_3C{=}C(H)C(H){=}N\text{-}c\text{-}Hex]_2} \rightleftharpoons \underset{\mathbf{1c}}{2Ru_4(CO)_{10}[CH_3C{=}C(H)C(H){=}N\text{-}i\text{-}Pr][CH_3C{=}C(H)C(H){=}N\text{-}c\text{-}Hex]} \quad (2)$$

separation of the obtained reaction mixture on a RP column gave three components in a roughly 1:2:1 ratio. The first and the last component were analyzed as **1a** and **1b**, respectively, both as 1:1 mixtures of two diastereomers. The second component was unambiguously characterized as an approximately 1:1 mixture of two diastereomers of the mixed ligand cluster $Ru_4(CO)_{10}[CH_3C{=}C(H)C(H){=}N\text{-}i\text{-}Pr][CH_3C{=}C(H)C(H){=}N\text{-}c\text{-}Hex]$ (**1c**) by FD mass and ^1H NMR spectroscopy. The formation of a mixed ligand complex by this route indicates that the thermally induced isomerization proceeds *intermolecularly*, most probably via the intermediacy of dinuclear radicals with formula $[Ru_2(CO)_5(CH_3C{=}C(H)C(H){=}NR^2)]^\bullet$ (R^2 = *i*-Pr, c-Hex), formed after homolytic fission of the central intermetallic bond. Such reactivity has been established for the isolobal cyclopentadienyl analogues.[23]

A second isomerization route was found during a study of reactions of **1a** with CO under various conditions.[17] A pure diastereomer of **1a** [(CA/AC) or (CC/AA)] dissolved in benzene or chloroform is converted into a 1:1 mixture of both diastereomers (eq 1) within 15 min at ambient temperature after saturation of the solution with CO. Prolonged exposure of **1a** to CO causes further reactions to take place, with formation of the CO adducts $Ru_4(CO)_n[CH_3C{=}C(H)C(H){=}N\text{-}i\text{-}Pr]_2$ (n = 12–14).[17] We examined the behavior of a mixture of **1a** and **1b** under CO as well. In this case, however, the mixed ligand complex **1c** was not formed (eq 2), indicating that the CO induced isomerization does, in contrast to the thermally induced isomerization, proceed *via* an *intramolecular* pathway.

Solid-State Structure of the *cis*-(CC/AA)-$Ru_4(CO)_{10}[CH_3C{=}C(H)C(H){=}N\text{-}i\text{-}Pr]_2$. The X-ray crystal structure of this diastereomer provides an unambiguous answer with respect to the configurations of the outer Ru atoms[14] and implies in conjunction with ref 10 that both diastereomers (CA/AC)-**1** and (CC/AA)-**1** exist. As the space group is $P2_1/a$, both the *cis*-(AA) and the *cis*-(CC) enantiomers of $Ru_4(CO)_{10}[CH_3C{=}C(H)C(H){=}N\text{-}i\text{-}Pr]_2$ (**1a**) are present in the crystal. The molecular geometry of the *cis*-(AA) enantiomer, along with the adopted numbering scheme is shown in a PLUTO drawing in Figure 3. Selected bond lengths and bond angles of *cis*-(CC/AA)-**1a** are listed in Table I. The molecule exhibits noncrystallographic C_2 symmetry, with the 2-fold axis running through the midpoint of the central Ru(2)–Ru(3) bond and perpendicular to the plane defined by Ru(2), C(5), Ru(3), and C(6).

The Ru(1)–Ru(2) and Ru(3)–Ru(4) bond lengths in *cis*-(CC/AA)-**1a** are comparable to those in *trans*-(CA/AC)-**1a**, whereas the central Ru(2)–Ru(3) bond length is slightly shorter in the former. The Ru(1)–Ru(2)–Ru(3) and Ru(2)–Ru(3)–Ru(4) angles deviate somewhat more from linearity than their counterparts in *trans*-(CA/AC)-**1a**, but the geometrical features of the MAD-yl ligands and their attachment to the linear Ru_4 skeleton closely resemble those in *trans*-(CA/AC)-**1a**.[10] Due to the relative cis orientation of the two η^5-azaruthenacyclopentadienyl rings in the *cis*-(CC/AA), the terminal CO ligands coordinated to Ru(2) and Ru(3) occupy mutual cis positions in *cis*-(CC/AA)-**1a**, as opposed to the mutual trans positions in *trans*-(CA/AC)-**1a**.

The dihedral angle between the planes defined by Ru(2), Ru(3), and C(5) and by Ru(2), Ru(3), and C(6) in *cis*-(CC/AA)-**1a** which amounts to 166° is comparable to the one found in *cis*-$[CpFe(CO)_2]_2$ of 164°.[24] In *trans*-(CA/AC)-**1a** and *trans*-$[CpFe(CO)_2]_2$ this angle is 180°, i.e., the central $M_2(\mu\text{-}CO)_2$ units are flat.

The molecular structure of *cis*-(CC/AA)-**1a** contains a compensating set of two asymmetric bridging CO ligands.[25] The Ru(2)–C(5) and Ru(3)–C(6) distances are about 0.1 Å longer

(23) Cutler, A. R.; Rosenblum, M. J. *Organomet. Chem.* **1976**, *120*, 87.

(24) Bryan, R. F.; Green, P. T.; Newlands, M. J.; Field, D. S. *J. Chem. Soc. A* **1970**, 3068.

(25) Lukehart, C. M. In *Fundamental Transition Metal Organometallic Chemistry*; Brooks/Cole: Monterey, CA, 1985; p 43.

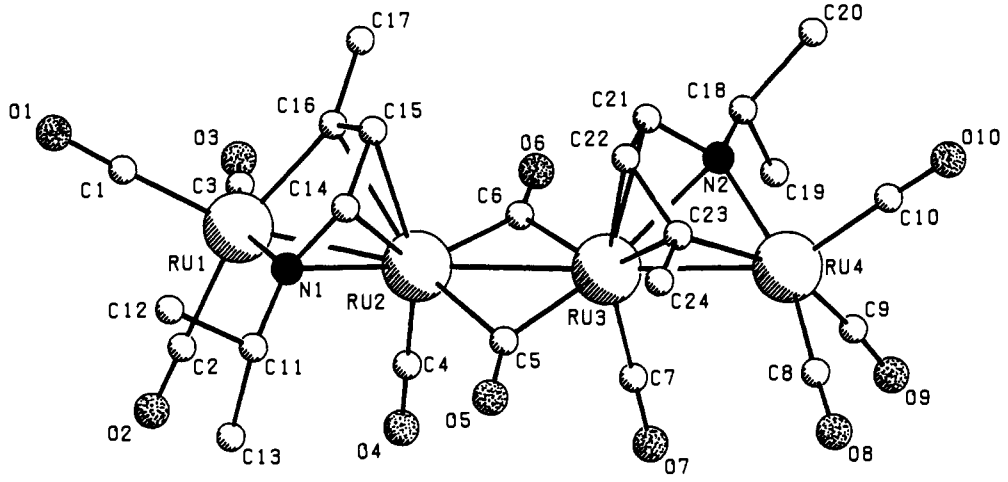

Figure 3. X-ray molecular structure of *cis*-(CC/AA)-**1a** (AA enantiomer).

Table II. ^{1}H NMR Data for (CA/AC)- and (CC/AA)-$Ru_4(CO)_{10}[C(H_\gamma)_3C{=}C(H_\alpha)C(H_{im}){=}NC(H_a)\{C(H_b)_3\}_2]_2$ (**1a**)[a]

solvent	compd	H_{im}	H_α	H_γ	H_a	H_b
C_6D_6	(CA/AC)-**1a**	6.05	4.82	2.60	3.13	1.09/0.74
	(CC/AA)-**1a**	6.03	4.81	2.59	3.14	1.17/0.85
$CDCl_3$	(CA/AC)-**1a**	6.82	5.08	2.55	3.53	1.25/1.17
	(CC/AA)-**1a**	6.73	5.10	2.60	3.52	1.30/1.18
CD_2Cl_2	(CA/AC)-**1a**	6.94	5.11	2.53	3.57	1.27/1.21
	(CC/AA)-**1a**	6.76	5.18	2.61	3.48	1.29/1.19
acetone-d_6	(CA/AC)-**1a**	7.55	5.44	2.49	3.69	1.31/1.26
	(CC/AA)-**1a**	7.27	5.69	2.65	3.48	1.21/1.13
CD_2Cl_2[b]	*cis*-(CA/AC)-**1a**	7.10	4.92	2.29	3.45 (br)	1.0–1.25 (br)
	trans-(CA/AC)-**1a**	6.77	5.02	2.46	3.45 (br)	1.0–1.25 (br)
CD_2Cl_2[c]	*cis*-(CC/AA)-**1a**	6.58	5.09	2.53	3.34	1.0–1.3 (br)
	trans-(CC/AA)-**1a**	6.95	4.99	2.44	3.53	1.0–1.3 (br)

[a] Measured in $CDCl_3$, 100 MHz, 298 K (unless stated otherwise), δ in ppm relative to Me_4Si; $^3J(H_{im},H_\alpha)$ = 2.0 Hz; $^4J(H_\alpha,H_\gamma)$ = 0.5 Hz; $^3J(H_a,H_b)$ = 6.5 Hz. [b] 173 K. [c] 183 K.

Table III. $^{13}C\{^1H\}$ NMR Data for (CA/AC)- and (CC/AA)-$Ru_4(CO)_{10}[C\gamma H_3C_\beta{=}C_\alpha(H)C_{im}(H){=}NC_a(H)\{C_bH_3\}_2]_2$ (**1a**)[a]

compd	C_{im}	C_α	C_β	C_γ	C_a	C_b	COs
(CA/AC)-**1a**[b]	130.0	104.2	197.2	32.8	62.8	29.5/26.5	224.1, 200.3, 195.8, 192.7
trans-(CA/AC)-**1a**[c]							249.4, 202.1, 201.3, 196.1[2]/196.0[6], 192.9
cis-(CA/AC)-**1a**[c]							252.8, 246.3, 202.8, 200.8, 196.1[2]/196.0[6], 193.1
(CC/AA)-**1a**[b]	129.7	103.9	197.2	32.9	62.7	29.4/26.5	223.8, 200.0, 195.5, 192.5
trans-(CC/AA)-**1d**[d]							200.4, 195.5, 192.4
cis-(CC/AA)-**1a**[d]							248.8, 202.4, 200.6, 195.7, 192.6

[a] δ in ppm relative to TMS in CD_2Cl_2 measured at 125.8 MHz. [b] 298 K. [c] 183 K. [d] 193 K.

than the Ru(2)–C(6) and Ru(3)–C(5) distances. A similar asymmetric central $Ru_2(\mu\text{-}CO)_2$ core is observed in the molecular structure of *trans*-(CA/AC)-**1a**, whereas regular symmetric planes have been observed in the molecular structures of *trans*-[CpRu-$(CO)_2]_2$,[26a] *trans*-[$(C_5Me_4Et)Ru(CO)_2]_2$,[26b] *trans*-[$CpFe(CO)_2]_2$,[27] and *cis*-[$CpFe(CO)_2]_2$.[24] In both diastereomers of **1a** the longer bonds in the $Ru_2(\mu\text{-}CO)_2$ unit are found opposite the η^2-coordinated C=C moieties. This asymmetry may be explained by considering the better π-acceptor properties of the π-coordinated C=C moieties of the two monoazadienyl ligands compared to the π-coordinated C=N moieties. So, except for the asymmetry within the central $Ru_2(\mu\text{-}CO)_2$ planes of both diastereomers of **1a**, the solid-state X-ray structures of the two diastereomers of **1a** corroborate the isolobal analogy between these tetranuclear complexes and their counterparts *cis*- and *trans*-$[CpM(CO)_2]_2$.

NMR Spectroscopy. The ^{1}H and ^{13}C NMR data of (CA/AC)-**1a** and (CC/AA)-**1a** in various solvents are listed in Tables II and III, respectively. The ^{1}H NMR spectra of both diastereomers at room temperature each show one set of mutually slightly different resonances indicating the presence of two magnetically equivalent 7e donating MAD-yl ligands in each diastereomer.

The ^{1}H NMR spectra show a pronounced solvent dependence. For instance, in C_6D_6 the H_{im} resonances of the (CA/AC) and (CC/AA) diastereomers of **1a** are found at 6.05 and 6.03 ppm, respectively, whereas in acetone-d_6 these resonances are observed at 7.55 and 7.27 ppm, respectively.

The ^{13}C resonances of the carbon atoms of the two MAD-yl ligands of both diastereomers of **1a** at 283 K are observed at similar chemical shifts and are consistent with the 7e donating σ-N, σ-C, η^2-C=N, and η^2-C=C coordination mode of these ligands. In the carbonyl region (298 K, 125.8 MHz) four resonances are observed in the terminal region (190–205 ppm), one of which originates from C_β and the other three from the CO ligands on the outer ruthenium atoms. Furthermore, one broad resonance is observed at about 224 ppm which originates from the four CO ligands of the central $Ru_2(CO)_4$ unit.

Fluxional Behavior of (CA/AC)-1a and (CC/AA)-1a in Solution. The 250.1-MHz ^{1}H NMR spectra of (CA/AC)-**1a** and (CC/AA)-**1a** in CD_2Cl_2 recorded at various temperatures are shown in Figures 4 and 5, respectively. This particular solvent was chosen because of a combination of favorable properties: good solvating properties, low freezing point, and an optimal dielectric

(26) (a) Mills, O. S.; Nice, J. P. *J. Organomet. Chem.* **1967**, *9*, 339. (b) Bailey, N. A.; Radford, S. L.; Sanderson, J. A.; Tabatabaian, K.; White, C.; Worthington, J. M. *J. Organomet. Chem.* **1978**, *154*, 343.

(27) Bryan, R. F.; Green, P. T. *J. Chem. Soc. A* **1970**, 3064.

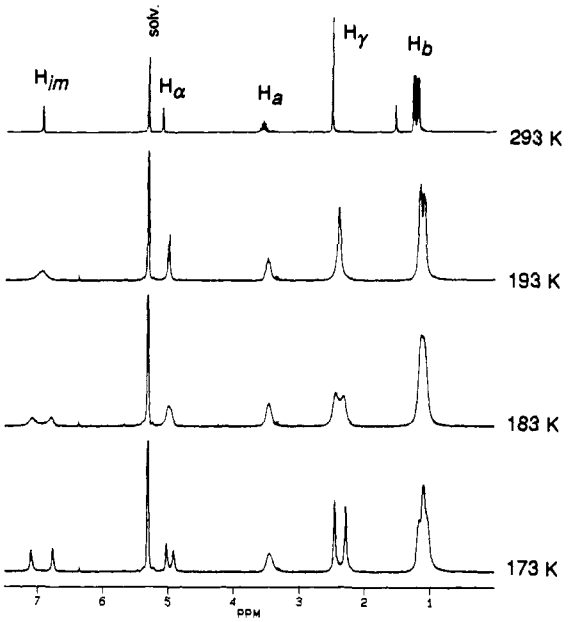

Figure 4. The 250.1 MHz ^1H NMR spectra of (CA/AC)-**1a** in CD_2Cl_2 as a function of temperature.

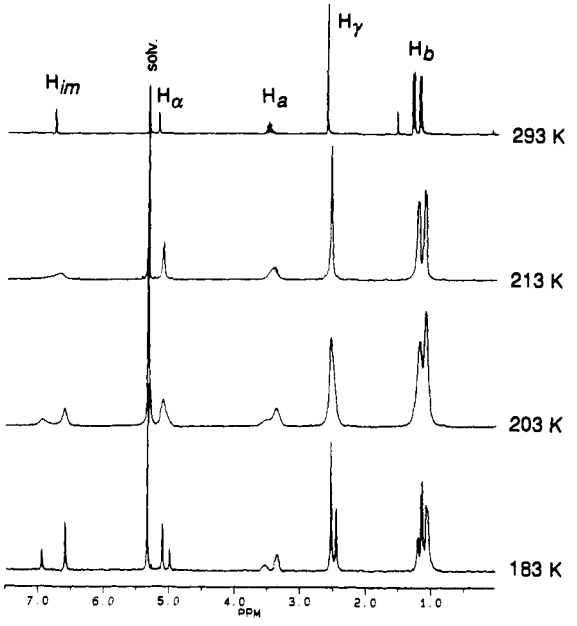

Figure 5. The 250.1 MHz ^1H NMR spectra of (CC/AA)-**1a** in CD_2Cl_2 as a function of temperature.

constant (ϵ = 9.1 at 20 °C) to study the fluxional processes. The ^1H NMR spectra recorded at 298 K show the presence of one set of resonances corresponding to two equivalent $CH_3C{=}C(H)C(H){=}N\text{-}i\text{-}Pr$ ligands present in each diastereomer. When the temperature is gradually lowered, the ^1H NMR resonances of both diastereomers broaden and ultimately appear as a double set of resonances at 173 K for (CA/AC)-**1a** and at 183 K for (CC/AA)-**1a**, respectively. This indicates that rapid cis/trans isomerization takes place between the cis/trans pairs of (CC)-**1a**, (AA)-**1a**, and (CA)-**1a**[14] (see Figure 3), respectively, in solution at 293 K, whereas these fluxional processes are slow on the NMR time scale at low temperature. The assignment of the four configurations, i.e., *cis*- and *trans*-(CA/AC)-**1a** and *cis*- and *trans*-(CC/AA)-**1a** has been based on the observed increase of the relative amount of the cis isomers after addition of a small amount of acetone-d_6 (ca. 20% v/v; $\epsilon \approx 20.7$ at 25 °C)) to the CD_2Cl_2 solutions (vide infra). For both diastereomers the cis/trans ratio observed at low temperature in CD_2Cl_2 differs from unity. The cis/trans ratio for (CA/AC)-**1a** at 173 K amounts to 0.95:1

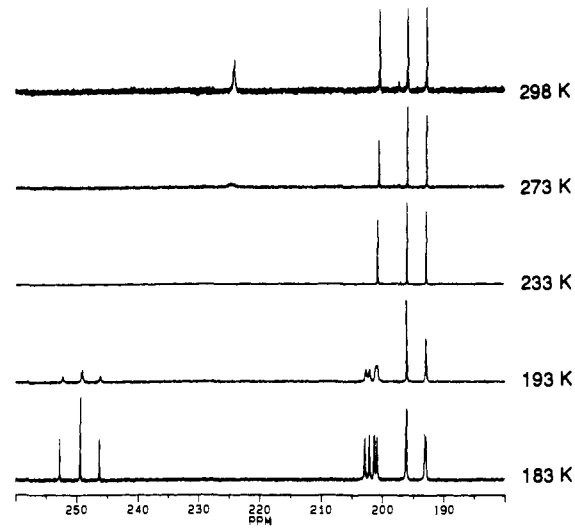

Figure 6. The 125.8 MHz ^{13}C NMR spectra of (CA/AC)-**1a** in CD_2Cl_2 as a function of temperature.

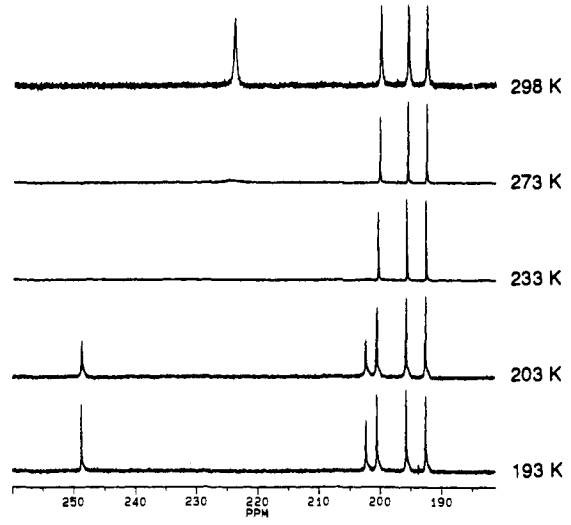

Figure 7. The 125.8 MHz ^{13}C NMR spectra of (CC/AA)-**1a** in CD_2Cl_2 as a function of temperature.

and for (CC/AA)-**1a** at 183 K to 2:1. From the coalescence temperatures of the imine, alkene, and methyl resonances, three independent estimates for the $\Delta G^\ddagger$ values[28] for cis/trans isomerization have been obtained for each diastereomer: $\Delta G_{av}^\ddagger$ (CA/AC)-**1a** = 38 kJ mol^{-1} and $\Delta G_{av}^\ddagger$(CC/AA)-**1a** = 42 kJ mol^{-1}.

For cis/trans isomerization in $[CpRu(CO)_2]_2$ a $\Delta G^\ddagger$ value of 29.4 kJ mol^{-1} has been reported.[5b] As the $\Delta G^\ddagger$ value found for the methyl substituted derivative $[(CH_3C_5H_4)Ru(CO)_2]_2$ of 39.5 kJ mol^{-1} is comparable to those found for the two diastereomers of **1a**,[5b] the higher $\Delta G^\ddagger$ values found for **1a** as compared to $[CpRu(CO)_2]_2$ might be ascribed to the presence of substituents on the azaruthenacyclopentadienyl rings in **1a**.

The CO regions of the 125.8 MHz ^{13}C NMR spectra of ^{13}CO enriched samples of (CA/AC)-**1a** and (CC/AA)-**1a** in CD_2Cl_2 recorded at various temperatures are shown in Figures 6 and 7, respectively. The occurrence of fluxional processes involving the bridging and terminal CO ligands of the central $Ru_2(CO)_4$ units in both diastereomers becomes already clear from the ^{13}C NMR spectra obtained at 298 K. The four CO ligands of the $Ru_2(CO)_4$

(28) $\Delta G^\ddagger$ was calculated by using the equation: $\Delta G^\ddagger = 19.14T_c(9.97 + \log T_c/\Delta\nu)$ (J mol^{-1}) where T_c is the coalescence temperature (K) and $\Delta\nu$ the shift difference (Hz) of the two exchange sites in the limiting low-temperature spectra. See: Günther, H. *NMR Spectroscopy, An Introduction*; Wiley: New York, 1973; p 243.

units of (CA/AC)-**1a** and (CC/AA)-**1a** appear as single broad resonances at 224.1 ppm and 223.8 ppm, respectively, intermediate between the regions where terminal and bridging CO ligands of ruthenium complexes are usually observed. Furthermore, three CO resonances are observed in the terminal region at 200.3, 195.8, and 192.7 ppm for (CA/AC)-**1a** and at 200.0, 195.5, and 192.5 ppm for (CC/AA)-**1a**, originating from the two equivalent $Ru(CO)_3$ units present in each diastereomer.[29]

Upon lowering the temperature of the sample of (CA/AC)-**1a**, the 224.1 ppm resonance first broadens and then disappears in the base line below 270 K. Upon further cooling to 183 K, three new resonances appear in the bridging region at 252.8, 249.4, and 246.3 ppm and two in the terminal region at 202.8 and 202.1 ppm, all belonging to CO ligands of the central $Ru_2(CO)_4$ units of *trans*- and *cis*-(CA/AC)-**1a**. Furthermore, the three resonances present in the terminal region at 298 K (200.3, 195.8, and 192.7 ppm) are split into three sets of two resonances at 183 K (201.3/200.8, 196.1[2]/196.0[6], 193.1/192.9 ppm). The $\Delta G^{\ddagger}$ value[28] of 39 kJ mol^{-1}, estimated for bridge/terminal exchange of the CO ligands in the central $Ru_2(CO)_4$ unit of (CA/AC)-**1a**, is comparable to the $\Delta G^{\ddagger}$ value of 38 kJ mol^{-1}, obtained for cis/trans isomerization of this diastereomer. The low-temperature ^{13}C NMR spectrum shows the presence of noninterconverting terminal and bridging CO ligands in the central $Ru_2(CO)_4$ units of both *cis*-(CA/AC)-**1a** and *trans*-(CA/AC)-**1a**. The three resonances in the bridging CO region can readily be assigned. Due to the presence of two *inequivalent* bridging CO ligands in *cis*-(CA/AC)-**1a**, the two resonances at 252.8 and 246.3 ppm will originate from *cis*-(CA/AC)-**1a** and the single resonance at 249.4 ppm originates from the two *equivalent* bridging CO ligands in *trans*-(CA/AC)-**1a**. Splitting of the ^{13}C resonances of the $Ru(CO)_3$ units at low temperature is consistent with the fact that cis/trans isomerization is slow on the NMR time scale and that the cis and trans forms of (CA/AC)-**1a** are present in approximately equal quantities in CD_2Cl_2 at 183 K. Addition of a small amount of acetone-d_6 caused an increase of the relative amount of the cis form of (CA/AC)-**1a**; at 183 K the cis/trans ratio in CD_2Cl_2 amounts to 0.95:1 and in CD_2Cl_2/acetone-d_6 (80/20) to 3:1. As expected because of its C_s symmetry, the cis configuration of (CA/AC)-**1a** is favored in more polar solvents over the trans configuration which is less polar.

At 193 K, the 223.8 ppm resonance of the other diastereomer, (CC/AA)-**1a**, has split into two resonances, one in the bridging CO region at 248.8 ppm and one in the terminal region at 202.4 ppm. The three resonances in the terminal region shifted to slightly higher δ values upon lowering the temperature but are still observed as three sharp signals. This resonance pattern suggests that only *cis*-(CC/AA)-**1a** is observed in the carbonyl region of the ^{13}C NMR spectrum at 193 K, as this configuration of (CC/AA)-**1a** contains two *equivalent* bridging CO ligands, which give rise to one resonance in the bridging region. Due to the presence of two *inequivalent* bridging CO ligands, two resonances should be observed in the bridging CO region (around 250 ppm) for *trans*-(CC/AA)-**1a** and four CO signals (one for the two equivalent terminal CO ligands of the central Ru centers and three for the two equivalent $Ru(CO)_3$ units) in the terminal region (190–205 ppm). Thus, *trans*-(CC/AA)-**1a** seems, according to the low temperature ^{13}C NMR spectrum, not to be present in the carbonyl region, although this configuration should be present in about 33% abundance according to the corresponding low-temperature ^1H NMR spectrum. Apparently, the terminal and bridging CO ligands in the central $Ru_2(CO)_4$ unit of *trans*-(CC/AA)-**1a** are in the intermediate exchange at 193 K. This situation corresponds to the behavior of the CO ligands in *cis*- and *trans*-$[CpFe(CO)_2]_2$ at 193 K but not to that in *cis*- and *trans*-$[CpRu(CO)_2]_2$, in which the CO ligands of both the cis and trans forms are assumed to be in the slow exchange when cis/trans isomerization is slow on the NMR time scale at 142 K.[5] The resonances of the carbonyl ligands of the equivalent $Ru(CO)_3$ units

(29) The fourth, less intense, resonance observed in this region at 197.2 ppm is attributable to the metalated C_β atom (see Table III).

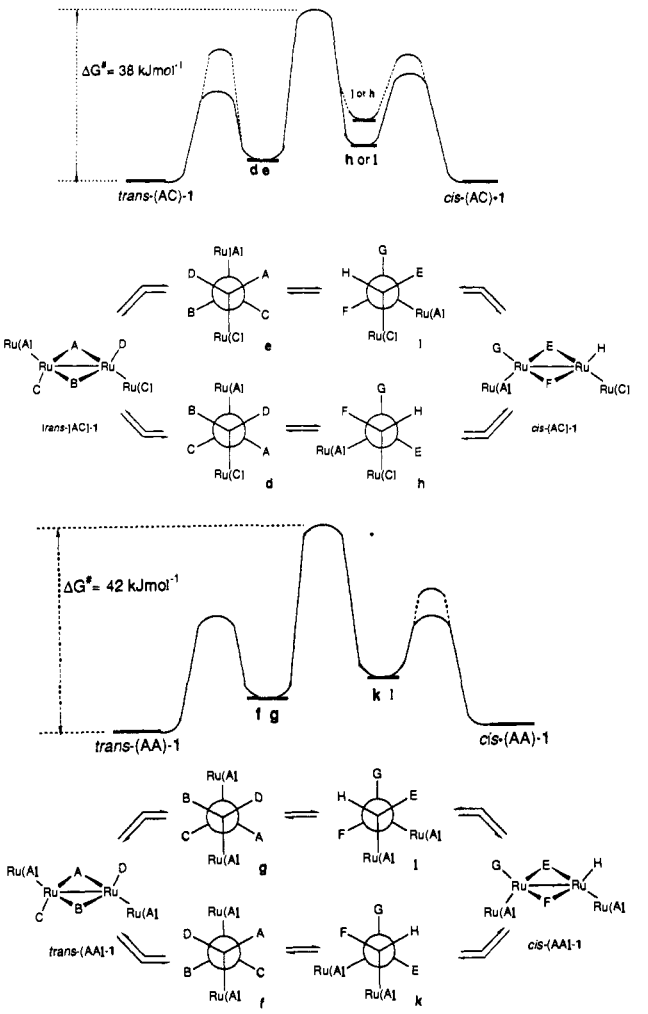

Figure 8. Qualitative profiles for the cis–trans isomerization of (CA)-**1a** and (AA)-**1a** and Newman projections of the nonbridged intermediates.

of *trans*-(CC/AA)-**1a**, however, should be observed separately from those of *cis*-(CC/AA)-**1a**, in the limiting low-temperature ^{13}C NMR spectrum, since these CO ligands do not participate in the fluxional process of the central $Ru_2(CO)_4$ unit. The only reasonable explanation for the fact that these do not appear separately is that the three COs of the $Ru(CO)_3$ units of *cis*-(CC/AA)-**1a** and *trans*-(CC/AA)-**1a** have, within experimental error, the same chemical shift ($\Delta\delta < 0.05$ ppm). Indeed, a ^{13}C NMR spectrum for (CC/AA)-**1a** recorded at 183 K in CD_2Cl_2 with a pulse delay of 60 s (thus allowing integration of the ^{13}CO signals) revealed that the five resonances at 248.8, 202.4, 200.6, 195.7, and 192.6 ppm integrate in a ratio of about 2:2:3:3:3, respectively, which is in agreement with coinciding resonances of the $Ru(CO)_3$ units of the cis and trans isomers and the relative amounts of ca. 2:1 as indicated by ^1H NMR (vide supra).

The intriguing question which arises is why do the CO ligands of the central $Ru_2(CO)_4$ unit in *trans*-(CA/AC)-**1a** not interconvert rapidly, whereas those in *trans*-(CC/AA)-**1a** do. The answer to this question lies in the diastereomeric nature of the complexes in the ground state and in the excited states due to the chirality of the two η^5-azaruthenacyclopentadienyl units present in each diastereomer. Pairwise opening of the CO bridges[3] in *trans*-(AC)-**1a** may lead to the nonbridged intermediates **d** or **e** and in *trans*-(AA)-**1a** to **f** or **g** (Figure 8).

Due to the presence of two chiral azaruthenacyclopentadienyl rings in **1a**, there will be a kinetic preference for the *equivalent asymmetric* bridging CO ligands A and B in *trans*-(AC)-**1a** to migrate to a specific ruthenium atom, thus forming either **d** or **e**. The synchronous back-formation of the two CO bridges has a similar preference, whereby the formerly bridging ligands A and B again form the CO bridges. Bridge/terminal CO exchange in

Table IV. IR Data for (CA/AC)- and (CC/AA)-$Ru_4(CO)_{10}[CH_3C{=}C(H)C(H){=}N\text{-}i\text{-}Pr]_2$ (**1a**)

compd	ν(CO), cm^{-1}						
(CA/AC)-**1a**[a]	2066.6 (s)	2005.2 (m)	1993.1 (s)	1951.5 (w)	1774.6 (m)		
(CA/AC)-**1a**[b]	2076 (sh)	2065 (vs)	2003 (s)	1991 (s)	1942 (w)	1794 (vw)	1762 (m)
(CA/AC)-**1a**[c]	2076 (sh)	2065 (vs)	2001 (sh)	1988 (s)	1963 (sh)	1939 (w)	1791 (vw)
	1753 (m)						
(CA/AC)-**1a**[d]	2074 (sh)	2065 (vs)	2003 (sh)	1994 (s)	1945 (sh)	1769 (m)	
(CA/AC)-**1a**[e]	2075 (sh)	2065 (vs)	1999 (sh)	1991 (s)	1964 (w)	1938 (vw)	1794 (vw)
	1756 (m)						
trans-(CA/AC)-**1a**[f]	2062 (s)	2008 (s)	1990 (vs)	1924 (s)	1758 (s)		
cis-(CA/AC)-**1a**[g]	2068 (s)	2058 (vs)	2008 (w)	1998 (vs)	1982 (vs)	1962 (m)	1950 (s)
	1779 (w)	1753 (s)					
(CC/AA)-**1a**[a]	2067.5 (s)	2006.5 (m)	1993.3 (s)	1949.7 (w)	1772.6 (m)		
(CC/AA)-**1a**[b]	2076 (sh)	2066 (vs)	2002 (sh)	1992 (s)	1940 (w)	1794 (vw)	1760 (m)
(CC/AA)-**1a**[c]	2076 (sh)	2066 (vs)	2001 (s)	1988 (s)	1964 (sh)	1937 (w)	1791 (vw)
	1752 (m)						
(CC/AA)-**1a**[d]	2074 (sh)	2055 (vs)	1994 (s)	1944 (w)	1769 (m)		
(CC/AA)-**1a**[e]	2075 (w)	2066 (vs)	1998 (s)	1991 (s)	1967 (w)	1935 (w)	1760 (m)

[a] In hexane, 293 K. [b] In dichloromethane, 273 K. [c] In dichloromethane, 178 K. [d] In 2-chlorobutane, 298 K. [e] In 2-chlorobutane, 143 K. [f] Hexagonally shaped crystals; in KBr pellet. [g] Rod shaped crystals; in KBr pellet.

trans-(AC)-**1a** can only take place via the intermediacy of *cis*-(AC)-**1a**, by rotation of one of the $[Ru(CO)_3(CH_3C{=}C(H)C(H){=}N\text{-}i\text{-}Pr)]Ru(CO)_2$ units in the nonbridged trans isomer by 120° with respect to the other, closing of the CO bridges giving *cis*-(AC)-**1a** and vice versa. Since this process requires additional energy, the exchange of the bridging and terminal CO ligands is frozen on the NMR time scale of *trans*-(AC)-**1a** at low temperature.

In *trans*-(AA)-**1a** (and *trans*-(CC)-**1a**), there is no preference for the two *nonequivalent symmetric* bridging CO ligands to migrate to either of the ruthenium atoms. Thus, the nonbridged intermediates **f** and **g** will be formed with equal probability. As the four terminal CO ligands in both **f** and **g** are equivalent, pairwise reclosing of the CO bridges by either the CO ligands A and B or C and D may take place. This nondiscriminating process accounts for the observed rapid exchange of the bridging and terminal CO ligands in the central $Ru_2(CO)_4$ unit of *trans*-(CC/AA)-**1a**.

The kinetic preference for bridge breaking/formation in *trans*-(CA/AC)-**1a** can be envisaged as follows. The distances of the bridging CO ligands to the bridged ruthenium centers, as observed in the crystal structure of *trans*-(CA/AC)-**1a**, are not equal,[10] so there will probably be a tendency for the asymmetric bridging CO ligands to migrate to the nearest ruthenium center during opening of these bridges. This leads to a kinetic preference for the formation of **d** over **e** by pairwise opening of the CO bridges in *trans*-(CA/AC)-**1a**.

Pairwise opening of the CO bridges in *cis*-(CA/AC)-**1a** leads to the diastereomerically related intermediates **h** and **i** (Figure 8). The barrier to diastereomer interconversion between these two will be very high, hence it is to be expected that bridge/terminal exchange will take place via the intermediates **d** and **e**, respectively, and *trans*-(CA/AC)-**1a**, similar to the findings by Farrugia et al. for $[CpFe(CO)_2]_2$.[6b]

As described in the introduction, cis/trans isomerization and bridge/terminal CO exchange in $[CpFe(CO)_2]_2$ have different kinetic barriers.[4] When isomerization is slow on the NMR time scale, the CO ligands in the cis isomer are static, whereas those of the trans isomer are still in the fast exchange, or, at lower temperatures, in the intermediate exchange. In contrast to the iron complex, cis/trans isomerization and bridge/terminal exchange in $[CpRu(CO)_2]_2$ are assumed to occur simultaneously.[5]

It has been reasoned by Gansow et al. that this difference in dynamic behavior is due to the metal involved, which was deemed to have a decisive influence on the kinetic barrier for bridge/terminal exchange in $[CpM(CO)_2]_2$ (M = Fe, Ru). According to this theory, bridge/terminal exchange in ruthenium carbonyl systems can only take place in conjunction with cis/trans isomerization, but not as an independent process occurring in the trans isomer solely.[30] Hence, *trans*-(CC/AA)-**1a** represents the first bis(dicarbonyl-(pseudo)cyclopentadienyl ruthenium) system in which the bridging and terminal CO ligands do exchange without concomitant cis/trans isomerization.

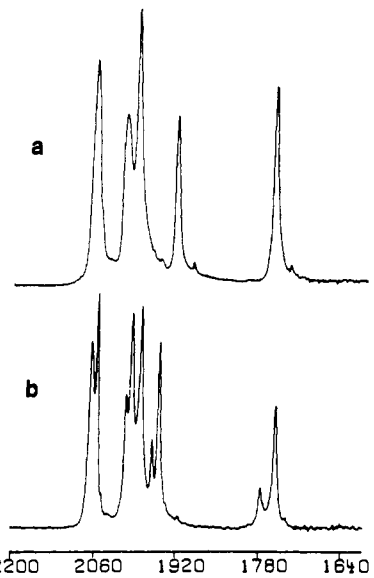

Figure 9. Solid-state IR spectra (KBr, CO stretching region) of *trans*-(CA/AC)-**1a** (a) and *cis*-(CA/AC)-**1a** (b).

IR Spectroscopy. The data from FT-IR spectra of pure (CA/AC)-**1a** and (CC/AA)-**1a**, which have been recorded both in solution (hexane, 2-chlorobutane, dichloromethane) and in the solid state (KBr), have been compiled in Table IV. For centrosymmetric (C_i) *trans*-(CA/AC)-**1a** five (four in the terminal and one in the bridging CO region) and for C_s symmetric *cis*-(CA/AC)-**1a** a maximum of ten absorption bands can be expected.

In the solid state, the IR spectrum of (CA/AC)-**1a** depends on the way by which the solid material has been obtained. When a hexane or toluene solution of (CA/AC)-**1a** is evaporated to dryness, *trans*-(CA/AC)-**1a** (five bands, see Figure 9a) was present solely. However, when crystallized from dichloromethane/hexane at −80 °C the IR spectrum of (CA/AC)-**1a** in KBr indicated the presence of a mixture of *trans*-(CA/AC)-**1a** and *cis*-(CA/AC)-**1a**. The two different crystal types, hexagonal

(30) A possible explanation is that the interpretation of the low-temperature ^{13}C NMR spectrum for $[CpRu(CO)_2]_2$ is not correct. This spectrum shows only one set of ^{13}CO signals, one in the terminal region and one in the bridging region, which were proposed to be composed of accidentally overlapping resonances of the cis and trans isomers of $[CpRu(CO)_2]_2$. However, this spectrum may alternatively be interpreted as showing merely the CO ligands of *cis*-$[CpRu(CO)_2]_2$, which are in the slow exchange, whereas those of *trans*-$[CpRu(CO)_2]_2$ remain unobserved because they are in the intermediate exchange.

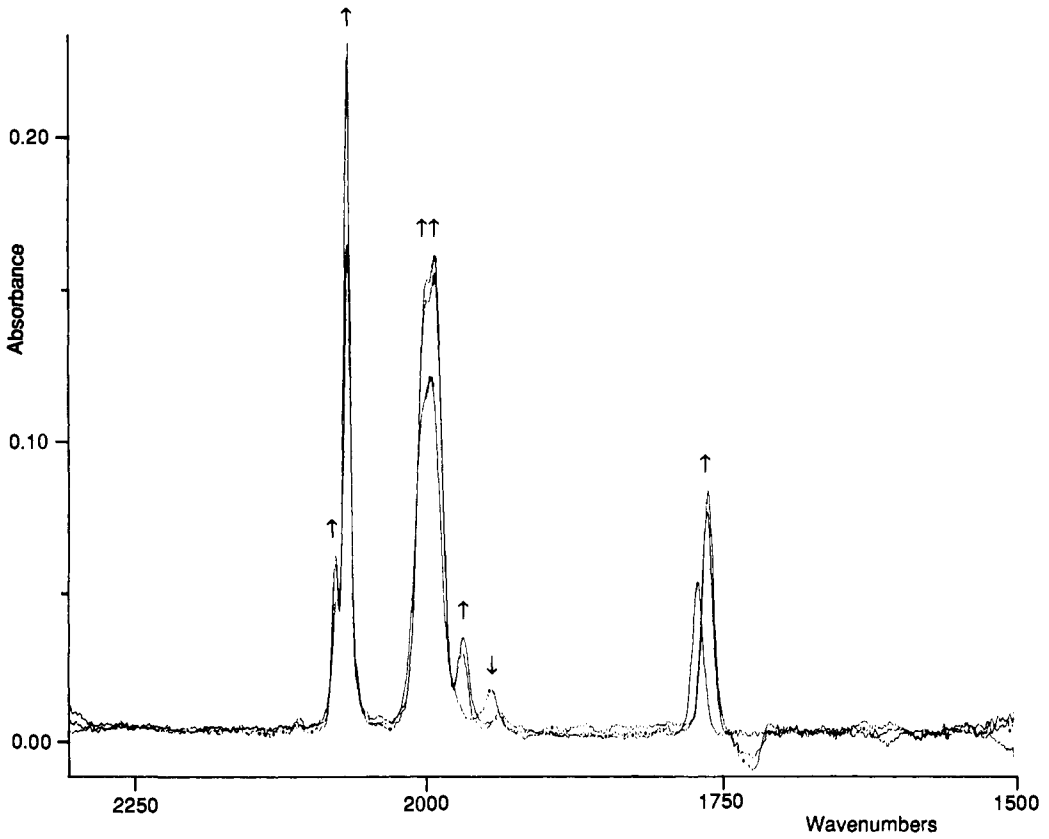

Figure 10. Solution IR spectrum of (CA/AC)-**1a** in 2-chlorobutane at 298, 143 and 133 K.

plates and rod shaped plates present in the crystalline material, were separated. In KBr, the hexagonal plates gave an IR spectrum similar to the one shown in Figure 9a, corresponding to *trans*-(CA/AC)-**1a**. The rod shaped crystals, however, gave a very different IR pattern (nine bands), which is shown in Figure 9b and which can be ascribed to *cis*-(CA/AC)-**1a**.[31]

In solution the IR spectrum of (CA/AC)-**1a** depends on the polarity of the solvent and on the temperature. In hexane (ϵ = 1.89) at room temperature the IR spectrum of (CA/AC)-**1a** indicates the presence of the trans isomer solely. In 2-chlorobutane (ϵ = 7.39) at room temperature, the spectrum shows the five bands corresponding to *trans*-(CA/AC)-**1a** along with a small shoulder at 2074 cm^{-1} which can be ascribed to *cis*-(CA/AC)-**1a** (see Figure 10). Upon lowering the temperature to 143 K, the intensity of the shoulder at 2074 cm^{-1} increases and two new bands, which are also ascribed to *cis*-(CA/AC)-**1a**, appear at 1964 and 1794 cm^{-1}. The band at 1938 cm^{-1}, which belongs to the trans isomer, decreases upon lowering the temperature. These spectra clearly indicate that at room temperature in 2-chlorobutane *trans*-(CA/AC)-**1a** is the dominant species over *cis*-(CA/AC)-**1a**, whereas at 143 K the reverse is observed. In dichloromethane the bands are broader due to solvent/compound interactions and therefore the cis/trans interconversion taking place upon lowering the temperature is less clearly visible than in 2-chlorobutane. However, from NMR studies (vide supra) it is known that in dichloromethane at about 180 K the cis and trans isomers are present in about equimolar amounts.

The IR spectra of (CC/AA)-**1a** in solution (hexane, 2-chlorobutane, and dichloromethane) are very similar to those of (CA/AC)-**1a** (Table IV.)[32] The IR spectrum of solid (CC/AA)-**1a** also depended on the way by which the solid material was prepared and indicated the presence of varying amounts of cis and trans isomers.[33]

It appears that the variation in the cis/trans ratio observed in solutions of both diastereomers of **1a** are very much the same to those observed for $[CpFe(CO)_2]_2$;[6] (i) the cis forms are preferred in more polar solvents and (ii) the cis/trans ratio increases upon lowering the temperature.

IR spectra of $[CpRu(CO)_2]_2$ in hydrocarbon solvents at room temperature show the presence of both bridged and nonbridged forms in an approximately 20:80 ratio.[34] However, there appears to be a general tendency that, upon increasing the size and number of substituents attached to the cyclopentadienyl rings the carbonyl-bridged configurations become more favored. As the azaruthenacyclopentadienyl rings in **1a** may be envisaged as cyclopentadienyl rings bearing several substituents, the presence of mainly carbonyl-bridged species **1a** in solution is in line with this tendency.

Conclusion

We have established for the first time that cis/trans isomerization and CO bridge-terminal exchange can be two independent

(31) Two absorption bands are present in the bridging region of *cis*-(CA/AC)-**1a**, a strong band at 1753 cm^{-1} and a weak band at 1779 cm^{-1}, which correspond to the symmetric and antisymmetric stretching vibrations of the two bridging CO ligands. The two bands at 1962 and 1950 cm^{-1} originate from the two terminal CO ligands present in the central $Ru_2(CO)_4$ unit. (These bands have shifted to considerably higher frequencies compared to 1924 cm^{-1} as is found for *trans*-(CA/AC)-**1a**. This shift will be the result of a less good π-overlap between the CO π^*-orbital and the relevant ruthenium d-orbital. This overlap depends on the angle θ(Ru–Ru–CO), which amounts to 94.65 (14)° in the *trans*-(CA/AC) isomer. Although we do not have an X-ray crystal structure of the *cis*-(CA/AC) isomer, θ in this isomer will be comparable to θ found in *cis*-(CC/AA)-**1a**, which amounts to 98.7 (4)° (mean). A larger deviation from 90° implies a less good π-overlap between inner ruthenium atoms and the terminal CO ligands, which is in concert with the observed increase in the vibrational energy of the inner terminal CO ligands on going from the *trans*-(CA/AC) to the *cis*-(CA/AC) diastereomer.)

(32) Although due to C_2 symmetry of *trans*-(CC/AA)-**1a** a maximum of ten bands can be expected, only five have been observed, just as for *trans*-(CA/AC)-**1a**.

(33) Solid material obtained after evaporation of an acetone or methanol solution of (CC/AA)-**1a** gave an IR spectrum (KBr) in which nine bands could be distinguished: 2071 (s), 1964 (sh), 2002 (s), 1988 (w), 1981 (w), 1971 (vs), 1955 (w), 1804 (m), 1753 (s). We tentatively assign these bands to *cis*-(CC/AA)-**1a**.

(34) (a) Bennett, M. A.; Bruce, M. I.; Matheson, T. W. In *Comprehensive Organometallic Chemistry*; Wilkinson, G., Stone, F. G. A., Abel, E. W. Eds.; Pergamon Press: Oxford, 1982; Vol. 4, pp 823 and 824 and references cited therein. (b) McArdle, P.; Manning, A. R. *J. Chem. Soc. A* **1970**, 2119.

processes in bis(dicarbonyl-(pseudo)cyclopentadienylruthenium) systems. Cis/trans isomerization was shown to occur in both diastereomers (CC/AA)-**1a** and (CA/AC)-**1a**, and the ratio of the cis and trans configurations is dependent on the polarity of the solvent and the temperature.

Acknowledgment. The authors thank Dr. D. J. Stufkens for helpful discussions and G. Schoemaker and D. Heijdenrijk for technical assistance. Several NMR spectra have been obtained at the National SON HF NMR facility at Nijmegen, The Netherlands. Part of this work was supported by the Netherlands Foundation for Chemical Research (SON) with financial aid from the Netherlands Organization for Scientific Research (NWO).

Supplementary Material Available: Tables of fractional coordinates, all bond lengths and angles, anisotropic thermal parameters of the non-H atoms, isotropic thermal parameters of the H atoms, and an ORTEP drawing of *cis*-(CC/AA)-**1a** (9 pages); listings of structure factor amplitudes (25 pages). Ordering information is given on any current masthead page.

Counterion Affinity Orders in Aqueous Micellar Solutions of Sodium Decyl Phosphate and Sodium Dodecyl Sulfate Determined by Changes in ^{23}Na NMR Relaxation Rates: A Surprising Dependence on Head Group Charge

Laurence S. Romsted* and Choon-Ock Yoon†

Contribution from the Department of Chemistry, Wright & Rieman Laboratories, Rutgers, The State University of New Jersey, New Brunswick, New Jersey 08903.
Received September 14, 1992

Abstract: Changes in quadrupole relaxation rates of ^{23}Na on addition of the Cl^- salts of Na^+, K^+, Rb^+, Cs^+, TMA^+, and TEA^+ ions were used to determine the relative affinities of these cations for micelles composed of the decyl phosphate monoanion, DPH^- (pH 5.3), the decyl phosphate dianion, DP^{2-} (pH 12.6), and their 1:1 mixture (pH 7.8) at 35 °C. Similar experiments were run in sodium dodecyl sulfate (SDS) micelles at 35 and 60 °C for comparison. The affinity of alkali metal ions for decyl phosphate micelles clearly increases with cation size at all three pH's. The alkali metal cations show significantly less affinity than TMA^+ and TEA^+ for DPH^- micelles and than TMA^+ for SDS micelles. In DP^{2-} micelles, the affinity order of the alkali metals remains the same, but surprisingly, TMA^+ and TEA^+ fail to displace Na^+ from the micellar interface. The 1:1 mixture of DPH^- and DP^{2-} shows intermediate behavior. These changes in affinity order with head group charge can be interpreted qualitatively by assuming that alkali metal ions are hydrated at the surface of decyl phosphate micelles but that they interact much more strongly with divalent than monovalent phosphate head groups, perhaps by site binding to the dianionic phosphate head group through an intervening water molecule. These results are compared with affinity orders of monovalent cations in solutions of micelles, vesicles, polyelectrolytes, DNA, and ion-exchange resins.

Introduction

Supramolecular aggregates and assemblies such as association colloids, vesicles, biological membranes, monolayers, proteins, DNA, polyelectrolytes, and ion-exchange resins all share an important structural feature, an interfacial region of moderate polarity (similar to that of alcohol) juxtaposed to a highly polar aqueous region.[1-14] Association colloids are dynamic aggregates of surfactants such as micelles, microemulsions, and reversed micelles which form homogeneous solutions spontaneously in water and in water and oil mixtures. Unlike polyelectrolytes and proteins, association colloids, monolayers, and biomembranes also have a substantial nonpolar region adjacent to the interfacial region which is composed of aggregated hydrocarbon chains and any added oil.[1,2,6,9-11] Aggregates with charged surfaces bind counterions selectively, and their solution properties such as aggregate size and shape, phase stability, the binding of ions and molecules, and their effects on the rates and equilibria of chemical reactions are sensitive to counterion concentration and type.[1,2,10,12,15-19] The relationship between an affinity order for a set of counterions and a particular aggregate property provides information on the nature of the interaction of counterions in the interfacial region, e.g., whether the counterions associated with the interface remain hydrated or are partially dehydrated and site-bound to surfactant head groups.[14,20-23]

Aqueous solutions of ionic micelles composed of surfactants with hydrocarbon tails of 8-18 carbons attached to cationic or

† Current address: Department of Chemistry, Kookmin University, 861-1 Chongnung-dong, Songbuk-gu, Seoul 136, Korea.

(1) Fendler, J. H. *Membrane Mimetic Chemistry*; Wiley-Interscience: New York, 1982.
(2) Bunton, C. A.; Nome, F.; Quina, F. H.; Romsted, L. S. *Acc. Chem. Res.* **1991**, *24*, 357.
(3) Forsen, S.; Brakenberg, T.; Wennerstrom, H. *Q. Rev. Biophys.* **1987**, *19*, 83.
(4) Manning, G. S. *Q. Rev. Biophys.* **1978**, *11*, 179.
(5) Manning, G. S. *Acc. Chem. Res.* **1979**, *12*, 443.
(6) *Surfactants in Solution*; Mittal, K. L., Ed.; Plenum Press: New York, 1989; Vol. 7.
(7) Israelachvili, J. *Intermolecular and Surface Forces*, 2nd ed.; Academic Press: London, 1991.
(8) Jain, M. K. *Introduction to Biological Membranes*, 2nd ed.; John Wiley & Sons: New York, 1988; p 423.
(9) *The Structure, Dynamics and Equilibrium Properties of Colloidal Systems*; Series C: Mathematical and Physical Sciences, Vol. 324; Bloor, D. M., Wyn-Jones, E., Eds.; Kluwer Academic Publishers: Boston, MA, 1990.
(10) *Physics of Amphiphiles: Micelles, Vesicles and Microemulsions*; Degiorgio, V., Corti, M., Eds.; Elsevier: Amsterdam, 1985.
(11) Tanford, C. *The Hydrophobic Effect: Formation of Micelles and Biological Membranes*, 2nd ed.; Wiley: New York, 1980.
(12) Cevc, G. *Biochim. Biophys. Acta* **1990**, *1031-3*, 311.
(13) Marcus, Y.; Kertes, A. S. *Ion Exchange and Solvent Extraction*; Wiley-Interscience: London, 1969.
(14) Reichenberg, D. In *Ion Exchange: A Series of Advances*; Marinsky, J. A., Ed.; Marcel Dekker: New York, 1966; Vol. 1, p 227.
(15) Lindman, B.; Wennerstrom, H. *Top. Curr. Chem.* **1980**, *87*, 32.
(16) Romsted, L. S. In *Surfactants in Solution*; Mittal, K. L., Lindman, B., Eds.; Plenum Press: New York, 1984; Vol. 2, p 1015.

0002-7863/93/1515-989$04.00/0